Free-space transmission with passive 2D beam steering for multi-gigabit-per-second per-beam indoor optical wireless networks

Research Article | Vol. 24, No. 17 | 22 Aug 2016 | OPTICS EXPRESS 19211

Optics EXPRESS

Free-space transmission with passive 2D beam steering for multi-gigabit-per-second per-beam indoor optical wireless networks

CHIN WAN OH,* ZIZHENG CAO, EDUWARD TANGDIONGGA, AND TON KOONEN

COBRA Institute, Eindhoven Univ. of Technology, P.O. Box 513, 5600MB Eindhoven, The Netherlands
**c.w.oh@tue.nl*

Abstract: In order to circumvent radio spectrum congestion, we propose an innovative system which can provide multiple infrared optical wireless beams simultaneously where each beam supports multi-gigabit-per-second communication. Scalable two-dimensional beam steering by means of wavelength tuning is proposed. A passive beam-steering module constructed with cascaded reflection gratings is designed for simultaneous multi-user coverage. We experimentally characterized the beam-steered system and thoroughly evaluated the performance of steered channels using the spectrally efficient and robust discrete multitone modulation in a bandwidth-limited system deploying 10 GHz telecom transceivers. This study reports the achievement of at least 37 Gbps free-space transmission per beam over a distance of up to 2 m over 5.61° × 12.66° scanning angles.

OCIS codes: (050.1950) Diffraction gratings; (060.2605) Free-space optical communication; (060.2390) Fiber optics, infrared.

References and links

1. S. Cherry, "Edholm's law of bandwidth," IEEE Spectr. **41**(7), 58–60 (2004).
2. M. Reardon, "Wireless spectrum: What it is, and why you should care," http://www.cnet.com/news/wireless-spectrum-what-it-is-and-why-you-should-care.
3. "The internet of things," http://share.cisco.com/internet-of-things.html.
4. G. Parodi, "Radio spectrum shortage prompts a growing number of initiatives," http://www.atelier.net/en/trends/articles/radio-spectrum-shortage-prompts-growing- number-initiatives_422770.
5. T. Kridel, "Cognitive Radio: A solution for the spectrum shortage?" http://www.lightreading.com/cognitive-radio-a-solution-for-the-spectrum-shortage/a/d-id/699609
6. T. McCall and M. Mahoney, "Spectrum of Issues," http://visual.ly/spectrum-issues.
7. L. Yang, "60 GHz: Opportunity for gigabit WPAN and WLAN convergence," ACM SIGCOMM Comput. Commun. Review **39**(1), 56–61 (2008).
8. J. M. Kahn and J. R. Barry, "Wireless infrared communications," in *Proceedings of IEEE* (IEEE, 1997), pp. 265–298.
9. H. Elgala, R. Mesleh, and H. Haas, "Indoor optical wireless communication: potential and state-of-the-art," IEEE Commun. Mag. **49**(9), 56–62 (2011).
10. K.-D. Langer and J. Grubor, "Recent developments in optical wireless communications using infrared and visible light," in *Proceedings of 9th International Conference on Transparent Optical Networks* (ICTON, 2007), pp. 146–151.
11. A. M. J. Koonen, "Optical Techniques for Gbps Wireless Indoor Access" in *Proceedings of International Topical Meeting on Microwave Photonics / 9th Asia-Pacific Microwave Photonics Conference* (MWP/APMP, 2014), pp. 403–408.
12. S. Koenig, D. Lopez-Diaz, J. Antes, F. Boes, R. Henneberger, A. Leuther, A. Tessmann, R. Schmogrow, D. Hillerkuss, R. Palmer, T. Zwick, C. Koos, W. Freude, O. Ambacher, J. Leuthold, and I. Kallfass, "Wireless sub-THz communication system with high data rate," Nat. Photonics **7**(12), 977–981 (2013).
13. Y. Wang, Y. Shao, H. Shang, X. Lu, Y. Wang, J. Yu, and N. Chi, "875-Mb/s Asynchronous Bi- directional 64QAM-OFDM SCM-WDM Transmission over RGB-LED-based Visible Light Communication System," in *Optical Fiber Communication Conference*, 2013 OSA Technical Digest Series (Optical Society of America, 2013), paper OTh1G–3.
14. G. Cossu, A. M. Khalid, R. Corsini, and E. Ciaramella, "Non-Directed Line-of-Sight Visible Light System providing High-Speed and Robustness to Ambient Light," in *Optical Fiber Communication Conference,* 2013 OSA Technical Digest Series (Optical Society of America, 2013), paper OTh1G–2.

#265209 http://dx.doi.org/10.1364/OE.24.019211
Journal © 2016 Received 16 May 2016; revised 30 Jun 2016; accepted 1 Jul 2016; published 10 Aug 2016

Optics EXPRESS

15. F. M. Wu, C. T. Lin, C. C. Wei, C. W. Chen, Z. Y. Chen, and K. Huang, "3.22-Gb / s WDM Visible Light Communication of a Single RGB LED Employing Carrier-Less Amplitude and Phase Modulation," in *Optical Fiber Communication Conference*, 2013 OSA Technical Digest Series (Optical Society of America, 2013), paper OTh1G–4.
16. D. Tsonev, H. Chun, S. Rajbhandari, J. J. McKendry, S. Videv, E. Gu, and D. O'Brien, "A 3-Gb/s Single-LED OFDM-Based Wireless VLC Link Using a Gallium Nitride," IEEE Photon. Technol. Lett. **26**(7), 637–640 (2014).
17. A. M. J. Koonen, "Fiber to the home/fiber to the premises: What, where, and when?" in *Proceedings of IEEE* (IEEE, 2006), pp. 911–934.
18. F. R. Gfeller, H. R. Nueller, and P. Vettiger, "Infrared Communication for In-House Applications," in *Proceedings of IEEE COMPCON* (IEEE,1978), pp. 132–138.
19. R. Ramirez-Iniguez and R. J. Green, "Indoor optical wireless communications." in *Proceedings of IEE Colloquium Optical Wireless Communications* (IEE, 1999), pp. 14/1–14/7.
20. K. Wang, A. Nirmalathas, C. Lim, and E. Skafidas, "High-speed duplex optical wireless communication system for indoor personal area networks," Opt. Express **18**(24), 25199–25216 (2010).
21. H. Al Hajjar, B. Fracasso, and D. Leroux, "Indoor optical wireless Gbps link dimensioning," in *Optical Fiber Communication Conference*, 2013 OSA Technical Digest Series (Optical Society of America, 2013), paper NTu3J–3.
22. H. Chen, H. P. A. van den Boom, E. Tangdiongga, and T. Koonen, "30-Gbps Bidirectional Transparent Optical Transmission with an MMF Access and an Indoor optical Wireless Link," IEEE Photon Technol. Lett. **24**(7), 572–574 (2012).
23. P. Brandl, S. Schidl, A. Polzer, W. Gaberl, and H. Zimmermann, "Optical Wireless Communication With Adaptive Focus and MEMS-Based Beam Steering," IEEE Photon. Technol. Lett. **25**(15), 1428–1431 (2013).
24. A. M. J. Koonen, C. W. Oh, and E. Tangdiongga, "Reconfigurable free-space optical indoor network using multiple pencil beam steering," in *Proceedings of 19th Optoelectronics and Communications Conference and the 39th Australian Conference on Optical Fibre Technology* (OECC/ACOFT, 2014), pp. 204–206.
25. C. W. Oh, E. Tangdiongga, and A. M. J. Koonen, "Steerable pencil beams for multi-Gbps indoor optical wireless communication," Opt. Lett. **39**(18), 5427–5430 (2014).
26. A. Gomez, K. Shi, C. Quintana, M. Sato, G. Faulkner, B. Thomsen, and D.C. O'Brien, "Beyond 100Gb/s indoor Wide Field-of-View Optical Wireless Communications," IEEE Photon Technol. Lett. **27**(4), 367–370 (2015).
27. C. W. Oh, E. Tangdiongga, and A. M. J. Koonen, "42.8 Gbps Indoor Optical Wireless Communication with 2-Dimensional Optical Beam steering," in *Optical Fiber Communication Conference,* 2015 OSA Technical Digest Series (Optical Society of America, 2015), paper M2F.3.
28. C. W. Oh, E. Tangdiongga, and A. M. J. Koonen, "Time-sharing resources for low cost and high performance indoor optical wireless networks," in *Proceedings of European Conference on Optical Communication* (ECOC, 2015), pp. 1–3.
29. W. Guo, P. Binetti, C. Althouse, L. A. Johansson, and L. A. Coldren, "InP Photonic Integrated Circuit with On-chip Tunable Laser Source for 2D Optical Beam Steering," in *Optical Fiber Communication Conference*, 2013 OSA Technical Digest (Optical Society of America, 2013), paper OTh3I.7.
30. H. Ishii, K. Kasaya, H. Oohashi, Y. Shibata, H. Yasaka, and K. Okamoto, "Widely Wavelength-Tunable DFB Laser Array Integrated With Funnel Combiner," IEEE J. Sel. Top. Quantum Electron. **13**(5), 1089–1094 (2007).
31. K. A. Mekonnen, C. W. Oh, Z. Cao, A. M. Khalid, N. Calabretta, E. Tangdiongga, and A. M. J. Koonen, "PIC-enabled Dynamic Bidirectional Indoor Network Employing Optical Wireless and Millimeter-wave Radio Techniques," in *Proceedings of European Conference on Optical Communication* (ECOC, 2016), (accepted).
32. K. Wang, A. Nirmalathas, C. Lim, and E. Skafidas, "Indoor Optical Wireless Localization System with Height Estimation for High-Speed Wireless Communications in Personal Areas," in *Proceedings of International Topical Meeting on Microwave Photonics,* (MWP, 2012), pp. 72–75.
33. P. Kułakowski, J. Vales-Alonso, E. Egea-López, and W. Ludwina, "Angle-of-arrival localization based on antenna arrays for wireless sensor networks," J. Comput. Electr. Eng. **36**(6), 1181–1186 (2010).
34. G. Cossu, M. Presi, R. Corsini, P. Choudhury, A. M. Khalid, and E. Ciaramella, "A visible light localization aided optical wireless system," in *Proceedings of 2nd IEEE workshop on optical wireless communications*, (IEEE, 2011), pp. 828–833.
35. F. Winkler and E. Fischer, E. Graß andG. Fischer, " A 60 GHz OFDM indoor localization system based on DTDOA," in *Proceedings of the 14th IST Mobile and Wireless Communications Summit* (IST SUMMIT, 2005). pp. 1–5.
36. K. Wang, A. T. Nirmalathas, C. Lim, and E. Skafidas, "Experimental Demonstration of Optical Wireless Indoor Localization System with Background Light Power Estimation," in *Optical Fiber Communication Conference),* 2015 OSA Technical Digest Series (Optical Society of America, 2015), paper W2A.63.
37. A. Gomez, K. Shi, C. Quintana, G. Faulkner, B. Thomsen, and D. C. O'Brien, "A 50 Gb/s Transparent Indoor Optical Wireless Communications Link With an Integrated Localization and Tracking System," J. Lightwave Technol. **34**(10), 2510–2517 (2016).
38. V. Nikulin, R. Khandekar, and J. Sofka, "Performance of a laser communication system with acousto-optic tracking: An experimental study," Proc. SPIE **6105**, 61050C (2006).

Optics EXPRESS

39. K. Van Acoleyen, K. Komorowska, W. Bogaerts, and R. Baets, "Integrated optical beam steerers," in *Optical Fiber Communication Conference,* 2013 OSA Technical Digest Series (Optical Society of America, 2013), paper OTh1B.6.
40. W. Guo, P. R. A. Binetti, C. Althouse, M. L. Mašanović, H. P. M. M. Ambrosius, L. A. Johansson, and L. A. Coldren, "Two-dimensional optical beam steering with InP-based photonic integrated circuits," IEEE J. Sel. Top. Quantum Electron. **9**(4), 6100212 (2013).
41. J. K. Doylend, M. J. R. Heck, J. T. Bovington, J. D. Peters, L. A. Coldren, and J. E. Bowers, "Two-dimensional free-space beam steering with an optical phased array on silicon-on-insulator," Opt. Express **19**(22), 21595–21604 (2011).
42. F. Vasey, F. K. Reinhart, R. Houdré, and J. M. Stauffer, "Spatial optical beam steerin with an AlGaAs integrated phased array," Appl. Opt. **32**(18), 3220–3232 (1993).
43. P. F. McManamon, P. J. Bos, M. J. Escuti, J. Heikenfeld, S. Serati, H. Xie, and E. A. Watson, "A review of phased array steering for narrow-band electrooptical systems," in *Proceedings of IEEE* (IEEE, 2009), pp. 1078–1096.
44. R. L. Forward, "Passive beam-deflecting apparatus", U.S. Patent No. 3612659 A, 1971.
45. Z. Yaqoob, M. A. Arain, and N. A. Riza, "High-speed two-dimensional laser scanner based on Bragg gratings stored in photothermorefractive glass," Appl. Opt. **42**(26), 5251–5262 (2003).
46. I. Filinski and T. Skettrup, "Fast dispersive beam deflectors and modulators," J. Quantum Electron **18**(7), 1059–1062 (1982).
47. N. A. Riza, "High speed optical scanner for multi-dimensional beam pointing and acquisition," in *LEOS'99 IEEE Lasers and Electro-Optics Society 1999 12th Annual Meeting* (IEEE,1999), pp. 70–71.
48. T. Chan, E. Myslivets, and J. E. Ford, "2-Dimensional beamsteering using dispersive deflectors and wavelength tuning," Opt. Express **16**(19), 14617–14628 (2008).
49. International Standard IEC 60825–1 © IEC: 1993 + A1:1997 + A2:2001: Safety of Laser Products – Part 1: Equipment Classification and Requirements. International Electrotechnical Commissions, Geneva (2001).
50. K. Schulmeister, R. Gilber, F. Edthofer, B. Seiser, and G. Vees, "Comparison of different beam diameter definitions to characterize thermal damage of the eye," Proc. SPIE **6101**, 61011A (2006).
51. "Technical note 6 Echelle gratings," http://www.gratinglab.com/Information/Technical_Notes/TechNote6.aspx
52. S. C. J. Lee, "Discrete multitone modulation for short-range optical communications," Eindhoven: Technische Universiteit Eindhoven, (2009).
53. K.-D. Langer, (2015), "DMT modulation for VLC. In: Shlomi Arnon (ed.) Visible Light Communication," (Cambridge: Cambridge University Press. Cambridge Books Online, 2015).
54. A. M. J. Koonen, C. W. Oh, K. Mekonnen, and E. Tangdiongga, "Ultra-high capacity indoor optical wireless communication using steered pencil beams," in *Proceedings of IEEE International Topical meeting on Microwave Photonics MWP 2015* (IEEE, 2015), paper WeC-5.
55. "Corning® SMF-28e+® Photonic Optical Fiber," Corning Incorporated (2010).

1. Introduction

Radio wireless communication is hitting the limits of its available spectrum. The increasing demand for high-speed wireless and on-the-spot applications has pushed the available radio frequency (RF) bandwidth to exhaustion [1,2]. In addition, the "Internet of Things" is leading to an exponential increase of connected devices up to a figure of 50 billion by year 2020, according to CISCO [3]. The high demand for connectivity will eventually lead to congestion in the wireless traffic causing lower channel throughput due to interference among devices and increase in wireless power consumption. Therefore, alternative means to accommodate the increasing wireless bandwidth demand are necessary [4,5]. There are several drawbacks in the current radio alternatives proposed, such as the high costs of acquisition of underused licensed sub-bands [6], and the limited bandwidth (only 7 GHz) of unregulated access provided by the Federal Communications Commission (FCC) in the 60 GHz radio spectrum [7]. Ultimately, the optical spectrum offers a more promising alternative as a substituting future-proof all-optical wireless solution or as a complementary solution to high speed radio wireless communication systems [8–12]. The optical spectrum offers bandwidths orders of magnitude higher than that available in the RF spectrum. The advantages of implementing optical wireless communication systems include not only the huge optical bandwidth available but also that it is unlicensed, physically secure as light waves do not penetrate walls, can offer spatial diversity that prevents multipath fading due to short carrier wavelength and large-area square-law detector [8], and absence of electromagnetic interference. However, for all intents and purposes, optical beams have to be compliant to skin- and eye-safety

Optics EXPRESS

regulations enforced by the American National Standards Institute (ANZI) Z136 and the International Electrotechnical Commission (IEC) 60825 standards for indoor use.

Recently, many research efforts have been and are being spent in the visible and infrared domain. Visible light communication (VLC) combines both illumination and communication functions via the usage of modulated light emitting diodes (LEDs). Due to the slow speed of illumination LEDs, mainly limited by its carrier recombination time in the semiconductor materials, VLC systems are fundamentally limited in bandwidth. At the moment, VLC bitrates have been demonstrated from a few 100s of Mbps [13,14], up to 3.22 Gbps, which wavelength division multiplexing (WDM) of RGB LEDs and carrier-less amplitude and phase (CAP) modulation are employed [15]. A 3 Gbps achievement with Gallium Nitride μLED employing OFDM format is the fastest speed recorded so far with a single LED [16]. Alternatively, infrared (IR) lasers, which are commonly employed in fiber optic communication in the telecom O-L bands, offer easy access and low cost by using readily available fiber communication devices. Such IR systems may seamlessly interface with fiber-to-the-home (FTTH) access networks [17]. They can offer a higher link power budget than VLC systems due to the relaxed eye-safety regulations for IR wavelengths (up to 10 mW power is permitted at $\lambda \geq 1400$ nm), and fundamentally higher photodetector sensitivity.

The use of IR communication for in-house applications has been first proposed in 1978 [18] and subsequently, several researchers in this area have published promising results of using diffused and direct beams for optical wireless communication [19–24]. In 1987, Bell Labs demonstrated a 1 mW OOK directed link with bitrate of 45 Mbps [19]. A line-of-sight (LOS) system employing steering mirrors with radio frequency for localization has been proposed in [20]. In [25], an LOS system with one-dimensional (1D) optical beam steering using passive gratings over a wavelength range between 1500 nm to 1630 nm with a steering angle of 17.16° has been demonstrated. Recently, in [26], Gomez et al. have proposed a two-dimensional (2D) beam-steering system using spatial light modulator (SLM) and by using a wavelength division multiplexing (WDM) of seven wavelengths from a seven channel Nyquist WDM transceiver and digital coherent system. As the SLM beam-steering module is based on active tuning, local powering will be required at each access point. In addition, software control is needed to adapt the blaze profile of the SLM. The SLM used has a steering angle of ± 3° and is used together with an angle magnifier to achieve ± 30°. Regarding scalability, an SLM-based steering module needs a specific carefully controlled setting per beam, necessitating accurate local control per beam generated from the remote central site, and handling multiple beams would imply a complex segmented SLM or multiple SLMs with associated comprehensive remote control issues.

In this paper, we propose and thoroughly evaluate a novel indoor system for optical wireless communication with 2D dynamic steering of high-capacity spatially confined pencil beams by employing cascaded reflection gratings at the access points and wavelength tuning elements at the central communication controller [27]. A steering coverage of 5.61° × 12.66° is achieved without angular magnification. No local control at the steering module is needed. We perform an analysis of the system which includes characterization of the spectral response, the beam profiles and the receiver's field of view (FOV). We further demonstrate transmission experiments using discrete multitone (DMT) modulation and analyze the high-speed performance of different wavelength channels (between 1530 nm and 1600 nm). This is the first time, to the best of authors' knowledge, that an indoor passive beam-steering system based simply on a passive structure of two reflection gratings for optical wireless communication is proposed with a full indoor architecture (with flexible backbone network, radio-over-fiber uplink and network control intelligence) and thoroughly evaluated not only with static characterization but also with data transmission.

The rest of this paper is arranged as follows: Section 2 describes the proposed system architecture; Section 3 explains the beam steering principle; Section 4 briefly discusses about

Optics EXPRESS

eye-safety; Section 5 contains the system characterization; Section 6 presents the transmission experiments and Section 7 presents conclusions.

2. Hybrid optical-radio wireless architecture

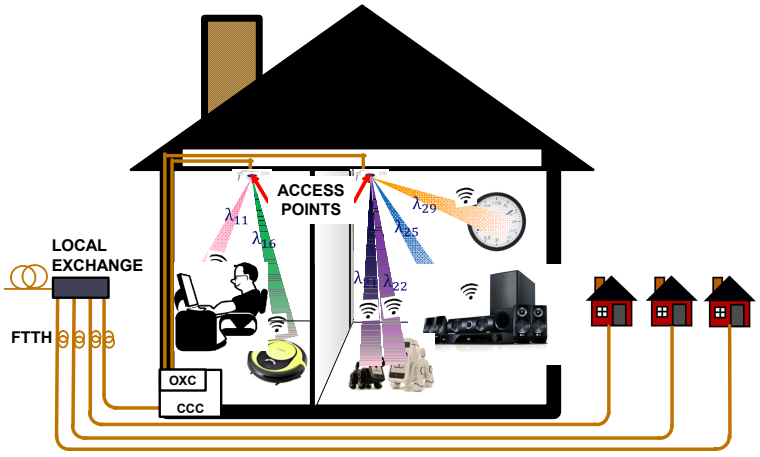

Fig. 1. Hybrid optical–radio wireless-equipped home with optical beam-steering modules at the access points and a central communication controller (CCC) interfacing the in-home and access networks. A tunable laser and an optical cross connect (OXC) provide and route wavelengths through the fiber backbone installed within walls/ceilings.

The architecture of the proposed solution for an indoor scenario is illustrated in Fig. 1. The system consists of free-space LOS optical beams for downlink and radio beams for uplink. Data signals are routed throughout the building via a fiber backbone network (fiber-in-the-home), which can be implemented with single-mode fiber (SMF) or multimode fiber and optical cross-connects (OXCs). Network protocols, routing logics and autonomous resource management will be localized at the central communication controller (CCC). The CCC will also act as the interface between the access network and the indoor network.

In each individual room, one or more access points (APs), each equipped with a beam-steering module termed as pencil radiating antenna (PRA), shall be implemented depending on the size of the coverage area. As we are working with LOS pencil beams for the downstream, beam steering is necessary in order to direct the LOS beams from the access point toward multiple users. Practical considerations for selecting a steering method include the ease of installation, enabling plug-and-play, without any local processing and without local powering. In order to maintain data integrity and speedy service provision for a group of users simultaneously with as low as possible transmission power, the beam-steering module has to be optimized for low-loss in the wavelength range of operation, has to be accurate, reliable, supports scalability, has to have high response speed, and a good coverage area. Taking into account these key requirements, we propose the use of passive diffraction gratings for beam steering in cooperation with remote wavelength-tuned source in the CCC.

The fundamental intention of the system is to provide a single beam to each single user. Providing multiple beams simultaneously requires multiple tunable lasers. This can obviously be realized by putting multiple tunable laser devices in parallel and combine their outputs onto the fiber feeding the PRA, or by an on-chip integrated array of tunable lasers. In such scenarios, several wavelengths can be provided simultaneously depending on the number of users in the room [28]. Tunable laser array and distributed feedback laser (DFB) diodes array have been reported in [29] and [30], respectively, with each enabling ≥ 30 nm tuning range. The selection of the source provision will depend on the timely progress and costs of these sources. Alternatively, to reduce the number of lasers needed and benefitting from the fast laser tuning times available, one may opt for a time-slotted system in which each user is

Optics EXPRESS

served by a specific wavelength during a specific timeslot and where the tunable laser is changing wavelength in the guard time between these timeslots.

Since typically the upstream speed is lower than the downstream (asymmetric network), radio technique is foreseen. On-going work is in progress in the 60 GHz domain. The 60 GHz signals can be sent via a radio-over-fiber technique back to the CCC. This configuration can be used together with a reflective semiconductor optical amplifier (R-SOA) or reflective electro-absorption modulator (REAM) to modulate the upstream data. Preliminary work with REAM is shown in reference [31].

In enabling mobility in the system, it is important that users are quickly localized in order to minimize connection latency. For this purpose, the use of radio and optical localization techniques [32–34] to locate and track the positions of the mobile devices are foreseen. A coarse localization is planned to be implemented with radio techniques. In [35], Winkler et al. has presented the capability of achieving accuracies of up to 50 cm using 60 GHz for localization. To complement the radio localization, fine-tuning shall be implemented optically by means of wavelength tuning and beam-manipulation. In [36], Wang et al. have demonstrated an average localization error of only 2.41 cm using background light power estimation. In [37], Gomez et al. have demonstrated localization and tracking with an accuracy of up to 2.5 mm using a CMOS camera at the base station observing LED IR tags at the nomadic terminal. As this topic is not within the scope of this paper, it will not be further detailed here.

Finally, in consideration of the higher eye-safety limit in the wavelength region of more than 1400 nm and to benefit from the already existing facilities used in the core, metro and access networks, the system is proposed to operate in the 1500 – 1600 nm telecom band. In due course, the advantages from the above wired-wireless indoor model are expected to emerge from its huge unlicensed bandwidth availability, high power efficiency and effective highly confined data beams, support of user-mobility, scalability in terms of data rate as well as its capability to accommodate the increasing number of users, provisioning of secure channels, mass availability of telecom band devices for ensuring cost effectiveness and higher link power budget compared to VLC systems.

3. Optical beam steering principle

In the implementation of such high bandwidth LOS narrow beams, beam steering is needed to direct each individual multi-wavelength pencil beam to a wireless device. Several free-space optical beam steering devices have been proposed in literature. These include micro-electro-mechanical mirrors [20,23], acousto-optic deflectors [38], on-chip grating modules [39–42] and liquid crystals [43]. However, these devices have drawbacks such as the need for local powering, slow steering speed, small steering angles and separate communication channels. To avoid these drawbacks, passive diffractive optics could play a major role in optical beam steering.

In 1971, R. L. Forward patented his invention on using an adjustable frequency beam generator to generate a collimated monochromatic beam and together with a Bragg scanning volume to deflect the beam into desired frequency dependent direction [44]. By using this technique, in 2003, Z. Yaqoob et al. [45] has demonstrated a 2D laser scanner using multiple photothermorefractive glass volumes (N) with each having multiple tilted Bragg-grating structures having optimal diffraction efficiency (M) are stacked together to achieve M × N 2D scanning. In 1982, I. Filinski and T. Skettrup [46] proposed a 1D light scanning by using dispersive optical components like prism, gratings, etc, together with electrooptical tuning of wavelength of broadband lasers. In 1999, N. A. Riza [47] demonstrated a 2D scanner using a mechanically tuned laser and a 1:4 WDM demultiplexer. An extension to the third dimension was made possible using GRIN lenses. More recently, in 2008, T. Chan demonstrated the combination of an array waveguide grating with a reflective grating [48]. However, the modules proposed in these literatures have not been demonstrated and evaluated for in-

Optics EXPRESS

building data communication feasibility where the capacity and distance (of several meters) are the important parameters.

The primary use of diffraction gratings is to disperse light spatially by wavelength. Therefore, a high bandwidth light source of which the wavelength can be tuned can definitely profit from the ability of the grating to diffract light into different spatial positions. These diffracted narrow beams could ultimately be used to carry information to users at various locations. The working principle of diffraction gratings is based on interference, whereby light waves interfere constructively and destructively forming distinct beams in certain directions. The locations of the bright spots are where light beams are diffracted to and these positions can be determined from the grating equation:

$$m\lambda = d(\mathrm{n}_1 \sin\theta_i \pm \mathrm{n}_2 \sin\theta_m) \tag{1}$$

where m is order of diffraction, λ is the wavelength of the beam, d is the period of the grating, θ_i the angle of incidence measured from grating normal, θ_m is the angle of transmittance or reflectance measured from grating normal and the variables n_1 and n_2 denote the refractive indices of the medium of incident light and the medium of transmitted or reflected light, respectively. The ± operation depends on the reference of the angle from the optical axis. Specular reflection of the grating is known as the zero-th order mode, which occurs at $\theta_i = \theta_m$, where most of the optical power is confined in. In order to optimize for maximum optical power in a desired diffraction order or angle, a blazed grating is used. Blazed gratings are designed for maximum efficiency at an order other than the zero-th order, with minimized residual power in all other orders. Blazed gratings which have a large blaze angle are known as echelle gratings.

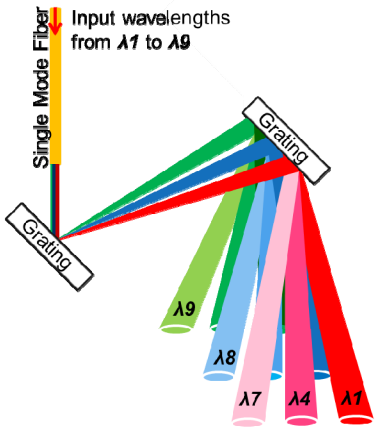

Fig. 2. 2D beam-steering concept. As an example in the figure, the first grating has an FSR of 3 wavelengths and the second grating provides at least three times the FSR of the first grating, thus, producing a cross dispersion effect.

In order to have a 2D area coverage and with a scanning functionality as proposed in this work, two gratings have to be orthogonally cascaded to each other [24]. The idea is that the first grating should have multiple times smaller free spectral range (FSR) than the second grating, as illustrated in Fig. 2. Therefore, in this work, two reflective echelle gratings, one which is blazed at 63° (blaze wavelength = 57 μm), ruled with 31.6 grooves/mm, and another blazed at 75° (blaze wavelength = 25 μm), ruled with 79 grooves/mm, are used for this feasibility study. The second grating has an FSR larger by twice that of the first grating, as illustrated in Fig. 3. The corresponding FSRs can be determined by the following equation:

Optics EXPRESS

$$FSR = \frac{\lambda_m}{m+1} \tag{2}$$

where λ_m refers to the wavelength operating in the order m.

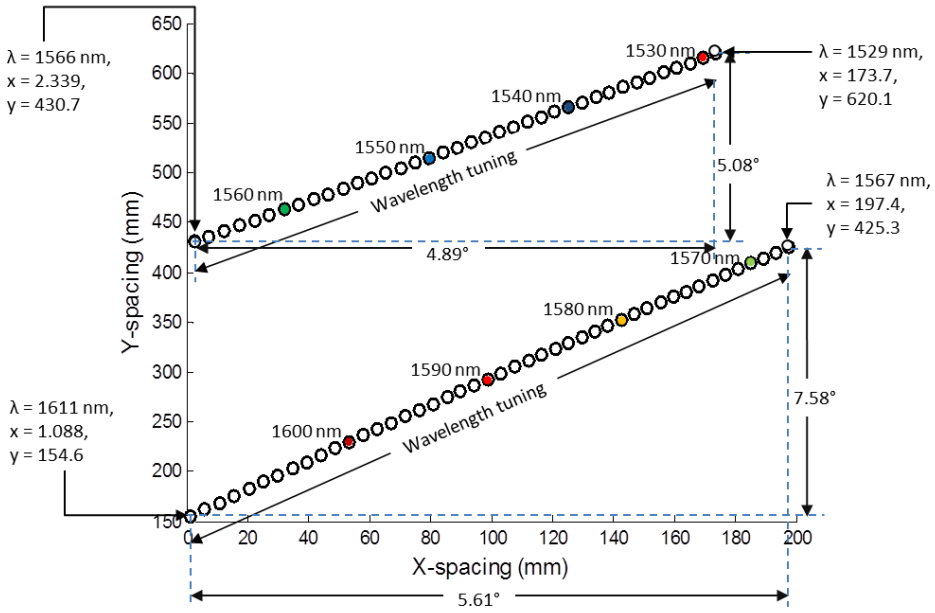

Fig. 3. Distribution of diffracted beams from a cross-mounted pair of reflection gratings (63° blazed with 31.6 grooves/mm and 75° blazed with 79 grooves/mm) over a wavelength range between 1529 nm and 1611 nm calculated for 2 m distance from the access point.

In practice, echelle gratings provide more than one diffraction order for each wavelength. For beam steering purpose, in order to avoid interference from the next diffraction order of the same wavelength, only one diffraction order of the second grating is used. In another situation, as shown in Fig. 3. we observe how the beams sweep across two different orders of the first grating when the wavelength is changed. This is due to the decreasing order (in integer) when the wavelength increases as can be derived from the blazed grating equation:

$$\begin{aligned} m\lambda &= 2d\sin\theta_m \\ (\frac{m}{2})(2\lambda) &= 2d\sin\theta_m \\ &\vdots \end{aligned} \tag{3}$$

$$(\frac{m}{n})(n\lambda) = 2d\sin\theta_m, n \text{ is an integer and } n \neq 0 \tag{4}$$

Correspondingly, the first grating has an FSR of 41 nm in order 36 and FSR of 44 nm in order 35, while the second grating has an FSR of 101 nm in order 15. In this scheme, by tuning the wavelengths of a tunable laser, which is located at the CCC, the different wavelengths are diffracted to the designated angles. Likewise, by using a first grating with much smaller FSR, a more compact distribution consisting of more scanning lines, can be achieved. From the figure, we see that by tuning the wavelengths over 1529 nm to 1611 nm, we achieve maximum steering angles of 5.61° × 12.66°. The scanning line between 1529 nm and 1566 nm gives an angular step of 0.19°/nm and scanning line between 1567 nm and 1611 nm gives

Optics EXPRESS

an angular step of 0.21°/nm. The spots tabulation of the cross-mounted gratings can be calculated by using the grating equation in the x- and y-axis:

$$\theta_{x,m} = \sin^{-1}(\sin\theta_{x,i} - \frac{m\lambda}{d_1}) \tag{5}$$

$$\theta_{y,m} = \sin^{-1}(\sin\theta_{y,i} - \frac{m\lambda}{d_2}) \tag{6}$$

where d_1 and d_2 are the period of grating 1 and grating 2, respectively.

4. Eye-safety

As the optical channels will be propagating in free space, it is a must that eye-safety is taken into account. The accessible emission limit (AEL) can be calculated as follows:

$$AEL = MPE \times \pi r^2 \tag{7}$$

where MPE (Maximum Permissible Exposure) [49] is the reference limit where a person can be exposed to without risk of injury, πr^2 is the beam area whereby the beam radius, r, is commonly calculated at 63% or 87% power level, i.e. at 1/e or $1/e^2$ [50].

In the transmission experiments in this paper, the collimators have a Gaussian beam diameter of 3.33 mm at 12.91 mm in front of the collimator housing. Using the well-known Gaussian equation, the radius at z-position away from the waist can be calculated using:

$$w(z) = w_o\sqrt{1+\left(\frac{z}{z_R}\right)^2} \tag{8}$$

where w_o is the Gaussian beam waist (radius), z is the distance considered and z_R is the Rayleigh range. For a direct point-to-point link, at 2 m distance, the radius is 1.767 mm, therefore, an area of 0.09813 cm^2. The AEL is then 0.1 W/cm^2 × 0.09813 cm^2 = 9.81 mW = 9.92 dBm and at 2.5 m distance, the AEL is 10.43 mW = 10.18 dBm.

As the experiments conducted are limited to a maximum of 9.2 dBm optical power transmitted into free space, all the beams are within the eye-safety limit.

5. System characterization

The objective of this section is to provide information of the system's bandwidth, beam size and receiver's FOV, which are key items impacting the system's performance. In Section 5.1, the spectral response of the system is measured in order to determine the bandwidth limitation that the steering module imposes on the free-space channels. In Section 5.2, the beam profile is measured. This will give us information of the beam size and profile as seen from the receiver's side. With this information, we show that all the beams are within the eye-safety limit. Lastly, in Section 5.3, we measured the collimator's tilt tolerance, illustrating how precise the steering system needs to be aligned. For practical reasons such as to enable user mobility and ease of channel establishment and reception, a receiver with a larger FOV will be necessary.

5.1 Spectral response

The spectral response profile of a system has a major impact on the bandwidth of the overall system, next to the bandwidth of the receiver. It is measured in a testbed constructed for 2D-diffracted transmission over 2 m, as shown in Fig. 4. Two methods of measurements have been considered. The first is by using a tunable laser to sweep the wavelength across the receiving (Rx) collimator whereby the power is then measured with a power meter. The

Optics EXPRESS

second method is carried out by transmitting amplified spontaneous emission (ASE) wideband signal originating from an erbium-doped fiber amplifier (EDFA) and the received beam is connected to an optical spectrum analyzer (OSA).

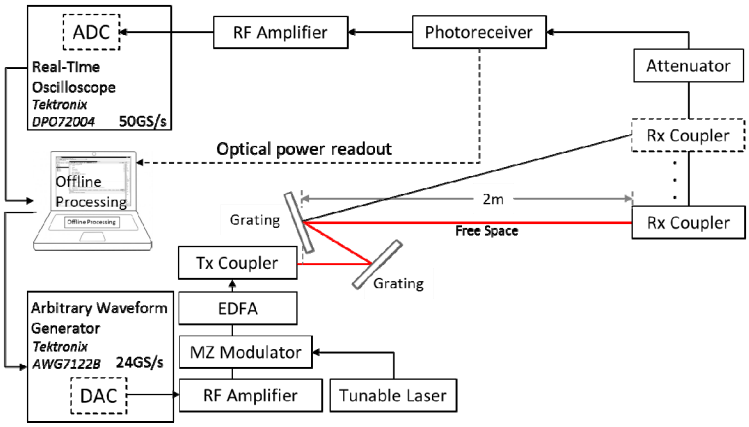

Fig. 4. Testbed setup for 2 m transmission with 2D steering for spectral characterization. Digital-to-Analog Converter (DAC), Analog-to-Digital Converter (ADC), Transmitting (Tx), Receiving (Rx), Mach-Zehnder (MZ), Erbium-doped Fiber Amplifier (EDFA), Radio Frequency (RF).

The transmitting (Tx) power, just before free space, is set to ≤ 9.2 dBm. The polarization controlled beam is transmitted to free space through a triplet lens collimator with a focal length of 18.36 mm and a full-angle divergence of 0.034°. The $1/e^2$ beam diameter is 3.33 mm at the focal plane. The beam hits the first echelle grating of 63° blaze angle at a near-Littrow angle. The grating grooves are aligned perpendicularly to the optical table. The second grating has a 75° blaze angle and is cascaded orthogonally to the first, so the grooves are aligned parallel to the optical table, creating a cross dispersion effect, as shown in Fig. 2. The free-space beam is then recoupled back into the SMF by means of another identical receiving (Rx) collimator. In the first method, the optical power detected at each position is then recorded as the wavelength is varied. For non-modulated signals, the DMT signal is turned off. These measurements are compared to the second method, in which the spectral response is measured using an OSA.

The optical power loss across the free-space system for wavelengths between 1530 nm and 1600 nm is between −13.5 and −16 dB (4.5% and 2.5% power efficiency, respectively) as shown in Table 1.

Table 1. Measured free-space loss at each wavelength position

Wavelength (nm)	Free-space Loss (dB)
1530	−14.8
1540	−13.5
1550	−13.7
1560	−15.7
1570	−16.8
1580	−16.0
1590	−15.8
1600	−16.0

Optics EXPRESS

The loss measured is the optical power difference measured just before the Tx lens collimator and right after the Rx lens collimator. The main contributions are from the collective losses of both gratings and alignment loss. The first grating, designated for blaze wavelength of 57 μm, operates at orders 35 and 36 while the second grating, designated for blaze wavelength 25 μm, operates at order 15. As blazed gratings are designed for maximum efficiency at the designated wavelengths, while the gratings here are used at much higher orders for wavelengths, between 1530 nm and 1600 nm, these gratings are not optimal in power efficiency but they provide the FSRs needed for the proof-of-concept demonstration of steering with cascaded gratings. The power efficiency of echelle gratings could typically achieve up to 50% −75% (less than 3 dB loss) [51] and with transmission gratings, efficiencies of over 90% (less than 0.5 dB loss) are achievable. As for the alignment, the collimators are very sensitive toward angular tilt, as will be discussed in section 5.3.

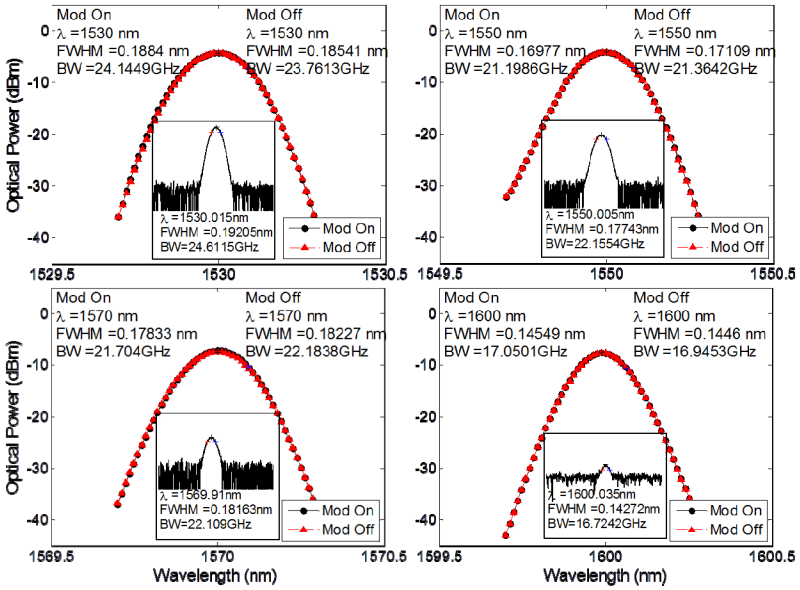

Fig. 5. Spectral responses of 2D beam-steered channels for wavelengths between 1530 nm and 1600 nm at 2 m. Modulation (Mod), wavelength (λ), Full Width at Half Maximum (FWHM), spectral bandwidth (BW).

Figure 5 shows the spectral response of the static channels (denoted by the red trangles) with wavelengths originating from the tunable laser. The spectral response recorded using the OSA (see inset) corresponds agreeably. In general, the measurements stay in good agreement for both measurement methods giving a range of spectral bandwidth between 16.7 GHz and 24.6 GHz for wavelengths between 1530 nm and 1600 nm.

As the cascaded gratings behave as a filter of approximately 20 GHz, the channels will be limited in bandwidth. In order to fully utilize the bandwidth for data transmission, the spectrum-efficient discrete multitone (DMT) modulation format can be used. Subsequently, we have evaluated what the impact of the DMT signaling on the system's spectral response is. We observe in Fig. 5 that when data modulation is turned on, the DMT signal shows negligible effect on the curves (denoted by the black circles).

5.1.1 Brief introduction to discrete multitone modulation

DMT is a variant of the orthogonal frequency division multiplexing (OFDM) technique and is widely used e.g. in copper-based Digital Subscriber Line (DSL) user access networks for high speed transmission. DMT is a baseband multicarrier and multiplexing modulation technique

Optics EXPRESS

that by its so-called bit-loading function can allocate the number of bits per subcarrier adapting to the signal-to-noise ratio (SNR) in order to optimize channel capacity in a transmission link. A rate-adaptive bit-loading algorithm is utilized to maximize the data rate over the available system bandwidth while maintaining the threshold for forward error correction (FEC) at a bit error rate (BER) ≤ 3.08×10^{-3}. The operation of DMT transmit (modulation) and receive (demodulation) blocks in the digital domain is shown in Fig. 6. From the transmitting end, a stream of serial input data is subdivided into parallel streams and modulated with quadrature amplitude modulation (QAM) mapping. The complex signal is then multiplied with its conjugate satisfying the Hermitian symmetry for real-valued inverse fast Fourier transform (IFFT) output. IFFT is performed to convert the signal into time domain. The signal is then converted from parallel streams to a single serial high-speed stream for transmission. At the receiving end, FFT is performed to demodulate the signal and the BER is calculated. For a more extensive treatment of DMT modulation techniques, please refer to [52,53].

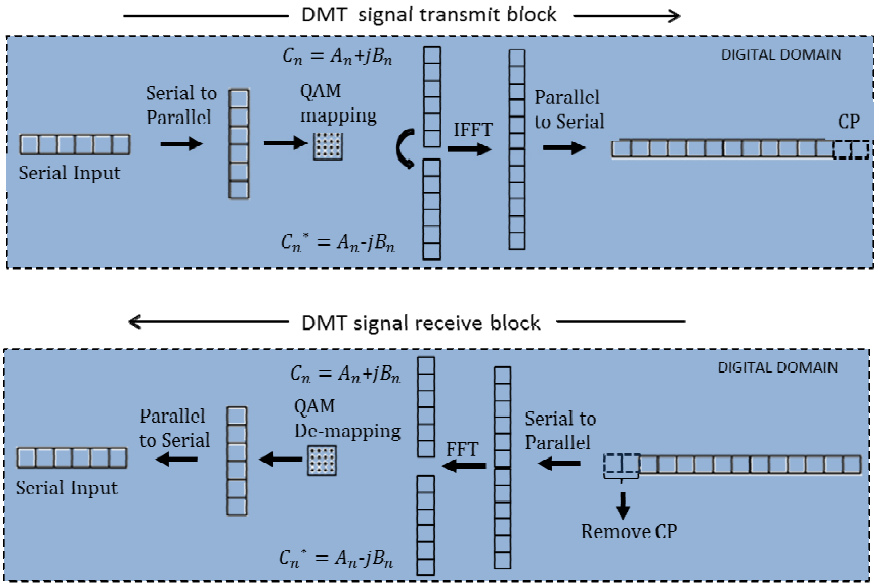

Fig. 6. Discrete multitone modulation (DMT) operation blocks for transmitting and receiving DMT signals. Quadrature Amplitude Modulation (QAM), Cyclic Prefix (CP).

5.2 Beam profiles

The transmit power, just before free space, is kept ≤ 9.2 dBm. The beam profiles of the 2D-steered beams have been measured by using a motorized arm to displace the position of the receiving lens in order to map the optical power over the beam. At 2 m distance, the profiles naturally give a larger beam diameter than at the originating beam waist which is 3.33 mm in diameter at 12.91 mm in front of the collimator housing. The full width at half maximum (FWHM) and $1/e^2$ (= reference point at the beam waist) can be obtained from the Gaussian profiles which are measured when the DMT modulation is turned on and turned off. This way, we can observe the effects of modulation on the dispersion and the size of the beam after transmission.

In Fig. 7, we observe that the FWHM and $1/e^2$ diameter remain consistent for all measurements. Between 1530 nm and 1600 nm, we measured FWHM values between 2.23 mm and 2.42 mm, and a minimum $1/e^2$ diameter between 3.76 mm and 4.11 mm. Modulating the beam does not affect the beam size, therefore, dispersion is negligible. Inserting the minimum $1/e^2$ beam radius of 3.76/2 = 1.88 mm, therefore, an area of 0.11 cm^2, into Eq. (7),

Optics EXPRESS

the AEL is then 0.1 W/cm^2 × 0.11 cm^2 = 11 mW = 10.41 dBm. With this higher accessible limit, these beams that arrive at the receiver are eye-safe. For practicality, the size of the eventual beam will depend on the effective area of the photodetector and the density of the diffracted spots. More analysis are given in [54].

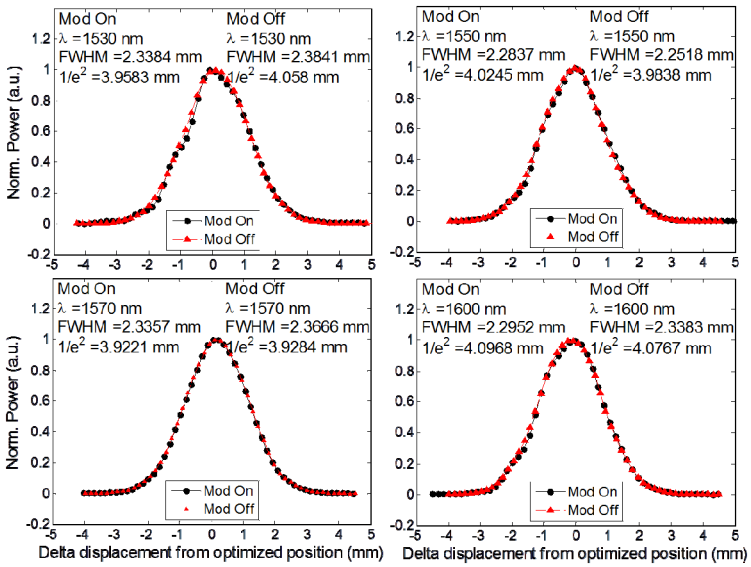

Fig. 7. Beam profiles of 2D beam-steered channels for wavelengths between 1530 nm and 1600 nm at 2 m. Modulation (Mod), wavelength (λ), Full Width at Half Maximum (FWHM).

5.3 Receiver's field of view

In the LOS system, alignment with the collimator is tedious due to the limited full-field of view (FFOV), which is related to the full-angle divergence, θ_{div}. The theoretical maximum is 0.034° at 1/e^2 using:

$$FFOV^{\circ} = \theta_{div}{}^{\circ} = \frac{MFD}{f} \times \frac{180}{\pi} \tag{9}$$

where MFD is the mode field diameter of SMF-28e + which is 10.4 ± 0.5μm at 1550 nm [55].

Optics EXPRESS

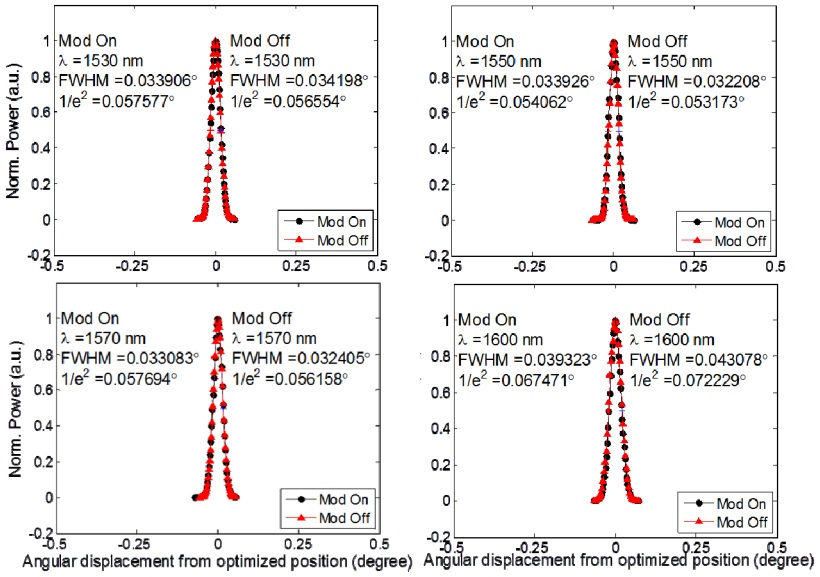

Fig. 8. Lens tilt tolerance measured with wavelengths between 1530 nm and 1600 nm. Modulation (Mod), wavelength (λ), Full Width at Half Maximum (FWHM).

Subsequently, we measured the extent of tilt for the collimators used in this experiment, as shown in Fig. 8. Measurements have been made for wavelengths between 1530 nm and 1600 nm, with and without DMT modulation. All the measured profiles match consistently, with FWHM angles between 0.032° and 0.043° and $1/e^2$ angles between 0.054° and 0.067°. The measurements show that the steering system is very precise. Although these collimators have excellent light collimation efficiency, with a loss of < 1dB over 2 m, their reception angle is very small, thus requiring tedious alignment at the receiving end. Therefore, it is vital to implement a small form factor receiver with larger FFOV in order to ease channel establishment and reception in a practical scenario.

6. Performance of 2D beam-steered channels with DMT signal transmission

In this section, we demonstrate a complete 2D beam-steered system using DMT signaling in a testbed constructed as illustrated in Fig. 4. The channel performances at different positions (by changing the wavelengths) are measured with the receiving collimators placed at various positions. These positions are compared to theoretically calculated spots as shown in Fig. 3 and the wavelengths are confirmed using the OSA.

The input data is generated with Matlab as a digitized DMT signal and an arbitrary waveform generator (AWG) is used to convert the DMT signal from digital-to-analog, which is then intensity-modulated onto the laser beam via a 10 GHz Mach-Zehnder modulator (MZM). The captured signal is received by a 10 GHz photoreceiver and then converted from analog-to-digital via the real-time oscilloscope (RTO) to be further processed offline with Matlab for obtaining the achievable data rates, BERs and constellations.

In an earlier work using a directly modulated DFB laser, we showed that the performance of an SMF link is quite comparable with that of a free-space channel of 2 m in a direct point-to-point link, as shown in Fig. 9. Therefore, in order to benchmark the measured results of the 2D-steered channels, a direct point-to-point free-space link with removed cascaded gratings in the setup in Fig. 4, is sufficient.

Optics EXPRESS

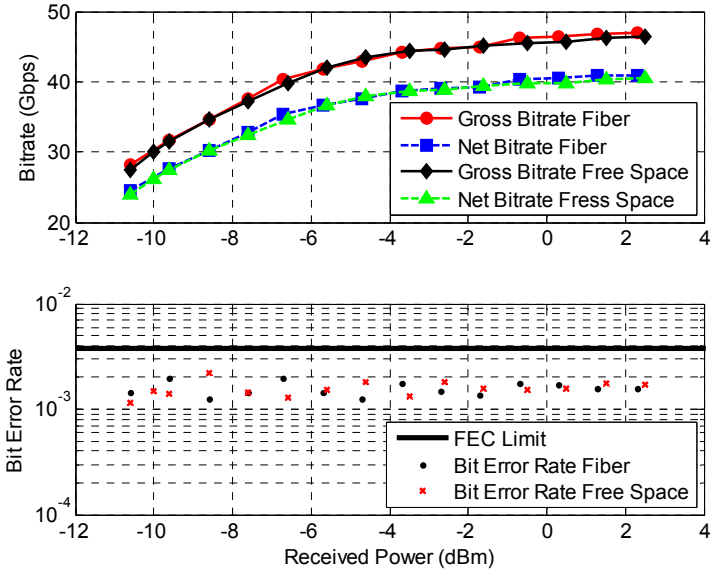

Fig. 9. The bitrate and bit error rate performance of an SMF versus direct point-to-point free-space link.

Figure 10 shows the comparison between the direct point-to-point free-space transmissions versus 2D-steered transmissions. We see that the measurements from the 2D-steered beams fall along the curve of the direct free-space transmission curve consistently at comparable received power levels. Thus, we can safely conclude that the steering module has negligible effect on the performance of the channels and that the steered channel performance is comparable to that of an SMF transmission link.

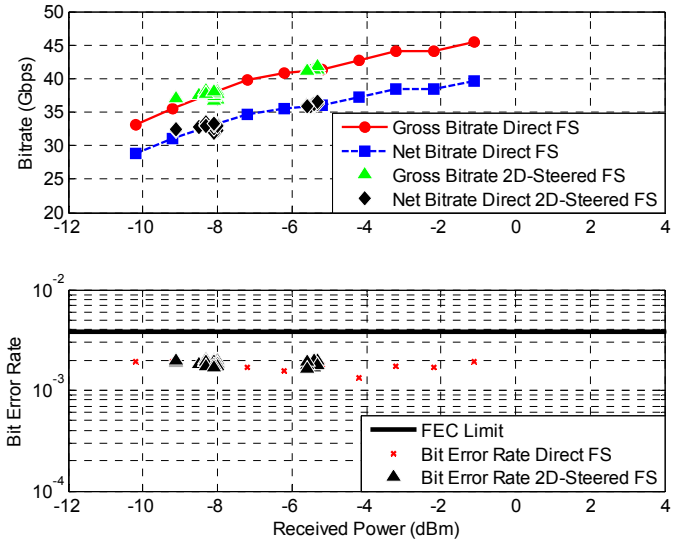

Fig. 10. Comparison between 2D beam-steered channels and direct point-to-point free-space (FS) channels for 8 wavelengths.

In Fig. 11, we report the achieved gross and net bitrates at different wavelengths. The net transmission bitrate is achieved after deduction of the cyclic prefix (guard against inter-frame interference due to channel dispersion), preambles (training and channel estimation) and 7% overhead for FEC coding from the gross bitrate. FEC coding is not implemented but is

Optics EXPRESS

considered and included in the calculation of bitrate. The highest bitrate achieved is at 1540 nm with a gross bitrate of 41.9 Gbps and net bitrate of 36.5 Gbps at −5.3 dBm. Each wavelength is represented with four measurements. All of the measured bitrates have a BER of less than 2×10^{-3} (within the FEC limit for error-free transmission with BER < 1×10^{-9}). The power is measured with an inline power meter set at 1550 nm. We observe that the data rates behave consistently with the power measurements.

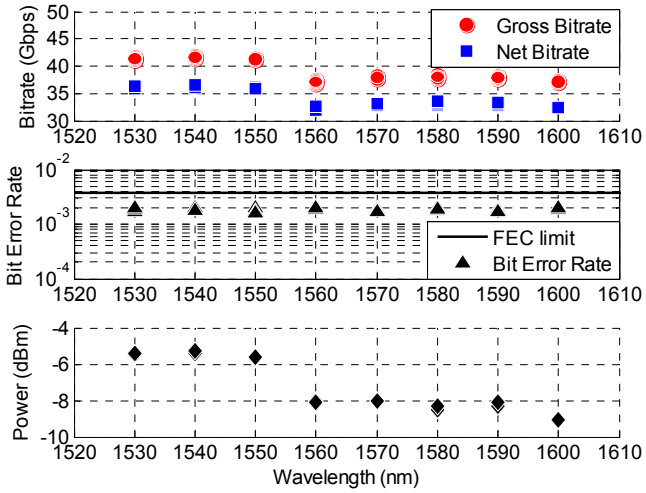

Fig. 11. Gross and net bitrates achievable with 2D beam steering with cross-mounted reflection gratings for wavelengths between 1530 nm to 1600 nm. The corresponding bit error rates and received optical powers are given.

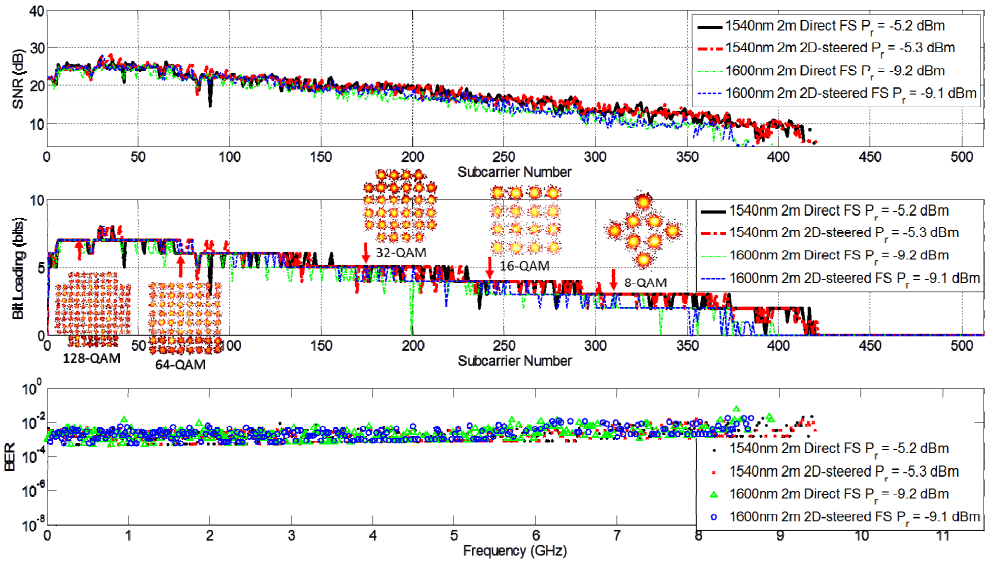

Fig. 12. Transmission of direct free-space (FS) point-to-point versus 2D steered channels. The Signal-to-Noise Ratio (SNR) bit loading at different subcarriers with constellation diagrams for received power, P_r = −5.3 dBm, and the BER of the different carrier frequencies at comparable received powers are plotted.

Figure 12 shows the SNR, bit loading for each subcarrier and the corresponding BER performance at the various subcarrier frequencies of the channel for 2D steered transmission measured at 1540 nm (with gross bitrate of 41.9 Gbps) and the worst channel measured,

Optics EXPRESS

which is at 1600 nm (with gross bitrate of 37.2 Gbps).These measurements are benchmarked to the corresponding free-space direct point-to point link measured at similar received power, i.e. −5.2 dBm and −9.2 dBm. Again, consistently matched curves are obtained.

Bit loading for 1540 nm direct point-to-point beam at −5.2 dBm is allocated up to 9.39 GHz compared to the 2D-steered beam at −5.3 dBm with up to 9.43 GHz. Bit loading for 1600 nm direct point-to-point beam at −9.2 dBm is allocated up to 8.9 GHz compared to the 2D steered beam at −9.1 dBm with up to 8.65 GHz. In general, up to a maximum 128 QAM levels were used with sporadic allocation of 256 QAM levels. As for BER performance, not all subcarriers achieved a BER $\leq 2 \times 10^{-3}$ but the average BER is still within the FEC limit for error-free transmission. Constellations corresponding to the loaded bits are shown for 1540 nm channel at a received power of −5.3 dBm. The constellations are clear and undistorted, and no amplitude nor phase noise is observed.

We have seen the feasibility of implementing the 2D beam steering using cross-mounted passive gratings with bitrates up to 41.9 Gbps (net 36.5 Gbps) at −5.3 dBm received power within 9.43 GHz bandwidth. With the consistently matched performance between fiber and free space, and between 2D beam-steered freespace and point-to-point direct free-space transmissions, we safely conclude that a fiber equivalent performance can be obtained with the 2D-steered free-space communication for indoors, implying that the passive steering module only introduces a very minor impact on the channel performance.

7. Conclusion

We have proposed and demonstrated a novel indoor optical wireless communication system employing 2D beam steering established by orthogonally cascading two passive reflection gratings. The optical beam-steering method does not require local powering while providing instantaneous remotely controlled steering by just wavelength-tuning of the signal. By steering the pencil beams to the required positions only, this method offers energy savings, secure communication and the ultimate capacity to individual users. This is the first time, to the best of authors' knowledge, that such an indoor system, with various architectural aspects taken into account, has been reported.

Free-space channel capacity per user of at least 37.2 Gbps up to 41.9 Gbps (between 1530 nm and 1600 nm) is measured over a free-space transmission distance of 2 m in a 10 GHz bandwidth-limited system. As demonstrated in the measurement results, the proposed optical wireless system has a comparable performance to that of an SMF transmission. Supposedly, by employing 8 wavelength sources with the minimum measured capacity of 37.2 Gbps per beam (out of 8 wavelengths' measurements), the system has the potential capability of supporting an aggregate capacity of at least 37.2 Gbps × 8 = 297.6 Gbps.

Even higher capacities can be achieved when the system's bandwidth is extended to 20 GHz or more; this prospect opens the road to provide beyond 100 Gbps wireless capacities per user. The system is also easily scalable by just adding wavelengths yielding additional beams, and thus, able to accommodate more users independently without affecting the channel capacity of other users. In short, the results indicate a promising potential of the proposed 2D-steered pencil-beam infrared optical wireless solution for the realization of future ultra-high capacity wireless indoor networks. The next major improvement steps include increasing the steering angle and beam size, and the implementation of localization functions and a wide angle receiver for easier alignment and signal reception.

Acknowledgment

This work is part of the Advanced Grant project Beam-steered Reconfigurable Optical-Wireless System for Energy-efficient communication (BROWSE), funded by the European Research Council within the FP7 program.